Soil-Structure Interaction (SSI) Analysis Using a Hybrid Spectral Element/Finite Element (SE/FE) Approach

P. Mirhashemian[1], N. Khaji[2*], and H. Shakib[3]

1. MSc in Earthquake Engineering, Civil Engineering Department, Tarbiat Modares University, Tehran, I.R. Iran
2. Associate Professor, Civil Engineering Dept., Tarbiat Modares University, Tehran, I.R. Iran, *Corresponding Author; email: nkhaji@modares.ac.ir
3. Professor, Civil Engineering Department, Tarbiat Modares University, Tehran, I.R. Iran

ABSTRACT

This study proposes a new formulation for modeling soil-structure interaction (SSI) problems. In this direct time-domain method, the half-space soil medium is modeled by spectral element method (SEM) which is based upon a conforming mesh of two-dimensional quadrilaterals, and the structural frame components are modeled by finite element method (FEM). Formulation and various computational aspects of the proposed hybrid approach are thoroughly discussed. To the authors' knowledge, this is the first study of a hybrid SE/FE method for SSI analyses. The accuracy and efficiency of the method is discussed by developing a two-dimensional SSI analysis program and comparing results obtained from the proposed hybrid SE/FE method with those reported in the literature. For this purpose, a number of soil-structure interaction and wave propagation problems, subjected to various externally applied transient loadings or seismic wave excitations, are presented using the proposed approach. Each problem is successfully modeled using a small number of degrees of freedom in comparison with other numerical methods. The present results agree very well with the analytical solutions as well the results from other numerical methods.

Keywords:
Soil-structure interaction;
Hybrid approach;
Spectral element method;
Finite element method;
Elastodynamics

1. Introduction

The dynamic response of massive structures, such as high-rise buildings and dams, may be influenced by soil-structure interaction as well as the characteristics of exciting loads and structures. The effect of soil-structure interaction is noticeable especially for stiff and massive structures resting on relatively soft ground. It may alter the dynamic characteristics of the structural response significantly. As a result, these interaction effects have to be considered in the dynamic analysis of structures in a semi-infinite soil medium [1].

Although a huge number of investigations have been conducted for soil-structure interaction analysis, depending on the modeling method for the soil region, all methods may be classified into two main categories. One method, the so-called direct method, evaluates the dynamic response of structure and its surrounding soil in a single analysis step, by subjecting the combined soil-structure system to a dynamic excitation. Another one which is termed as substructure method is based on the principle of superposition and the analysis is performed in several steps [2].

Various types of numerical methods such as finite element method (*FEM*), boundary element method (*BEM*), and hybrid techniques are commonly used to model soil-structure interaction effects. The use of *FEM* is advantageous as the procedures are versatile in nature and well-established (see for instance Refs. [3-6] among others). This method offers efficient advantages in the treatment of various aspects of soil domain such as arbitrary geometries, soil layering, material non-linearities, anisotropies and inhomogeneities. Nevertheless, due to its inherent difficulty in analyzing media of infinite extent, the radiation boundary conditions at infinity

have also been employed to overcome the problem of wave reflection and radiation on the far-field boundaries of the soil domain [7-10]. However, *FEM* remains a "computationally expensive" approach for elastody-namic and *SSI* problems [5, 11-13]. Apparently, one reason is that low-order *FEM* exhibit poor dispersion properties [14], while higher-order finite elements cause some troublesome problems like the occurrence of spurious waves.

Alternatively *BEM* which satisfies automatically the radiation boundary condition at infinity, requires substantially reduced surface discretizations even for 3*D* problems, and is appealing alternative to *FEM* for soil-structure systems [15-17]. However, *BEM* obviously suffers from two disadvantages. The first one is that although the coefficient matrix of the system is much smaller than those of *FEM*, this matrix is non-symmetric, non-positive definite and fully populated. The second disadvantage is that *BEM* is not appropriate in the treatment of material nonlinearities, anisotropies, and inhomogeneities of soil domain, and arbitrary complex half-space geometries.

Coupling finite element and boundary element methods retains the advantages of each method and eliminates their disadvantages. Various coupled *FE/BE* approaches have been suggested in the literature for problems in dynamic and seismic analysis of coupled soil-structure systems, see for example Refs. [18-24].

Spectral element method (*SEM*) provides a high-order technique, which allows obtaining the same accuracy as low-order methods (such as *FEM*) by using a reduced number of grid points, thus giving rise to a significant efficiency in computational resources. *SEM*, which enjoys all advantages of classical *FEM* (e.g., well-suited to handle complex geometries and nonlinear conditions), has been benefited by special sort of interpolation functions. These interpolation functions enable *SEM* to transfer a wide range of wavelengths through elements with higher accuracy and lower computational efforts compared to classical *FEM*. *SEM* which was originally introduced in computational fluid mechanics [25] is currently being implemented in elastodynamics problems, see for instance Refs. [26-28] among others. Nevertheless, little efforts have been achieved for the analysis of soil-structure systems using *SEM* [29].

In the past decade, *SEM*, which is especially appropriate for seismic wave propagation problems, has experienced significant developments. As a result, it seems that the soil-structure interaction while including the wave propagation considerations would be efficiently investigated by *SEM*. On the other hand, structural system effects may be accurately modeled using *FEM*. Consequently, a coupled *SEM-FEM* approach seems to exhibit an attractive and efficient tool for the soil-structure interaction analyses.

In this study, a combination of *SEM* and *FEM* is proposed for general two-dimensional analysis of soil-structure interaction problems under dynamic loading and elastodynamic problems. In order to obtain an approach applicable to nonlinear problems, a formulation that works directly in the time domain is developed. Employing the well-known direct method, the system is divided into a homogeneous, linear elastic half-space that is modeled using *SEM* and structural system, which is modeled by *FEM*. Before combining these two methods, *SEM* is verified by analyzing some example problems. The results obtained are compared with those from the literature. Afterwards, a soil-structure interaction model is developed by coupling the two methods. The coupled model is then applied to several numerical examples to illustrate how the *SE/FE* coupling may be achieved and how accurate the results are. It is found that the results agree well with the literature.

2. Problem Formulation

A numerical procedure based on the hybrid formulation, which combines *SEM* for the half-space soil domain and *FEM* for the superstructure is developed in the time domain, see Figure (1).

2.1. Spectral Element Method Formulation

In the early 1980s, spectral element method (*SEM*) was initially developed by Patera [30] in the field of fluid dynamics. This method was further developed and found many applications for modeling seismic wave propagation, e.g. [26-28]. In this section, a brief review of some important aspects of *SEM*, in particular those that would be subject to modification for their application to the coupled soil-structure system are briefly presented.

SEM is based upon a weak formulation of the equations of motion. This method combines the

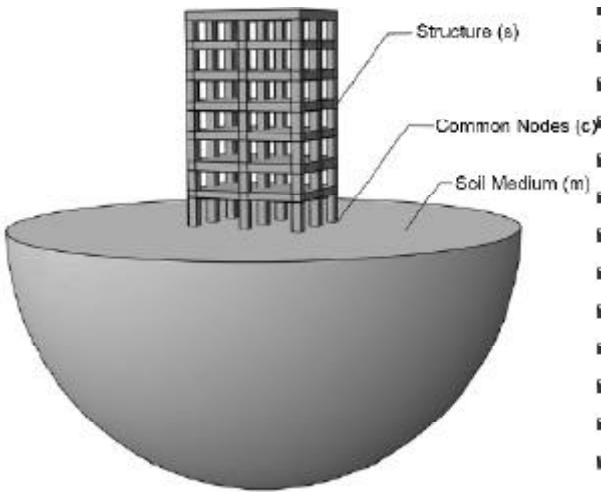

Figure 1. Soil-structure media.

flexibility of a finite element method with the accuracy of a pseudo-spectral method. Consequently, the *SEM* formulation process of stiffness and mass matrices is analogous to the classical *FEM* formulation. The main differences between *SEM* and *FEM* may be summarized in three main aspects: the polynomial degree of the basis functions, the choice of integration rule, and the nature of the time-marching scheme.

A crucial idea of *SEM* is adoption of specific shape/basis functions which is illustrated here as the first main difference between *SEM* and *FEM*. For any given quadrilateral element, the relation between a point displacement field $\vec{u}(\xi,\eta)$ within the element and a nodal point in the master square may be approximated as the following form:

$$\vec{u}(\xi,\eta)=\sum_{a=1}^{n_\ell+1} N_a(\xi,\eta)\vec{u}_a \tag{1}$$

where the local shape functions $N_a(\xi,\eta)$ are products of Lagrange polynomials, and $\vec{u}_a$ denotes nodal degrees of freedom. Firstly, the degree n_ℓ of the Legendre polynomials has to be chosen. The $(n_\ell+1)$ Lagrange polynomials of degree n_ℓ are defined in terms of $(n_\ell+1)$ internal local nodes $-1\le\xi_p\le 1$, $p=1,2,\ldots,n_\ell+1$. These local nodes are placed at special positions called Legendre-Gauss-Lobatto (*LGL*) points. These correspond, in a normalized 1*D* situation [-1, 1], to the zeroes of $P'_{n_\ell}(\xi)$, the first derivative of the Legendre polynomial of degree n_ℓ, and the extremes of the interval

$$\{zeros\ of\ P'_{n_\ell}(\xi)\}\cup\{-1,1\} \tag{2}$$

which means that one has $(n_\ell+1)$ *LGL* points for a polynomial of degree n_ℓ. By construction of a weak form (similarly as in *FEM*), element mass and stiffness matrices may be defined [31]. In other words, instead of using the strong form of the equations of motion, one can use an integrated form (i.e., weak form such as weighted residual approach). This is accomplished by weighting the equations of motion with an arbitrary test vector (the variation of displacement function is chosen here), integrating by parts over the domain volume, and imposing appropriate boundary conditions. To solve the weak form of the governing equations, integrations over the domain volume and boundary are subdivided in terms of smaller integrals over the volume and surface elements, respectively. Transformation to the global coordinate system and the assembly process are the same as in *FEM*. Finally, a wave propagation problem is reduced to the well-known ordinary differential equations, which can be written in a matrix form:

$$[M]\ddot{\vec{a}}+[C]\dot{\vec{a}}+[K]\vec{a}=\vec{F} \tag{3}$$

where [*M*], [*C*] and [*K*] are, respectively, the global mass, damping and stiffness matrices, and $\vec{F}$ is a vector of the time dependent excitation signal. The global matrices are equivalent to the sum of integrals over the set of the elements of the entire domain. They are built through the assembly process of the element matrices (direct stiffness method).

The second difference between *SEM* and *FEM* concerns to the numerical integration of element matrices. Let us consider the standard *FE* formulae of element characteristic matrices as:

$$\begin{aligned}[M^e]&=\int_{W_e}\rho[N]^T[N]dW\\ [K^e]&=\int_{W_e}[B]^T[D][B]dW\end{aligned} \tag{4}$$

in which [*B*] is strain-displacement transformation matrix, [*D*] denotes material stiffness matrix, [*N*] indicates shape function matrix, and ρ is the mass density. Each of integrations over the elements W_e are usually calculated by Gauss quadrature in *FEM*. In *SEM*, integrations may be approximated using the *LGL* quadrature rule instead

$$\int_{W_e} f(\vec{x})dxdy=\int_{-1}^{1}\int_{-1}^{1} f\left(\vec{x}(\xi,\eta)\right)J_e(\xi,\eta)d\xi d\eta\approx \sum_{p=1}^{n_\ell+1}\sum_{q=1}^{n_\ell+1}\omega_p\omega_q f_{pq}J_{e(pq)} \tag{5}$$

in which $f(\vec{x})$ indicates the integrand components of Eq. (4), ω_p and ω_q are the weights associated with the *LGL* points of integration, and $J_{e(pq)} = J_e(\xi_p, \eta_q)$ is the Jacobian of mapping from the element W_e to the reference domain. To integrate the functions and their partial derivatives over the elements, the values of the inverse Jacobian matrix need to be determined at the $(n_\ell + 1)^2$ *LGL* integration points for each element. The quadrature weights, which are independent of the element, are determined from the following equation:

$$\omega_a = \frac{2}{n_\ell (n_\ell + 1) P_{n_\ell}^2(\xi_a)}, \quad a = 1, 2, \ldots, n_\ell + 1 \tag{6}$$

As a result of the Lagrange interpolants selection at the *GLL* points, and its relation to the *GLL* integration rule, *SEM* shows an important property that leads to the diagonal form of the mass matrix, which allows a crucial reduction of the complexity and the cost of the algorithm [28]. In this manner, the diagonal mass matrix is obtained naturally in comparison with mass matrix lumping techniques, which incorporate considerable errors.

In order to take full advantage of the property described above, time-discretization of Eq. (3) is achieved based upon a Newmark scheme (central difference method) which, may be considered as the third difference between *SEM* and *FEM*. For *SEM*, this leads to simple explicit time schemes, as opposed to the numerically more expensive implicit time schemes used in *FEM* [31].

2.2. Coupled SEM-FEM Formulation

Formulation of equations of motion for a soil-structure interaction analysis has been frequently explained in the literature, see e.g. [1], and therefore is only briefly summarized in this section. Consider the dynamic response of a structure on a semi-infinite soil medium as shown in Figure (1) in which, the structure and soil media are to be modeled by *FEM* and *SEM*, respectively. Following a common notation used in the *SSI* literature, the nodes associated with the structure are identified with "*s*", those that lie along the soil-structure contact zone are "*c*" nodes, and the other nodes within the soil medium are identified with "*m*", see Figure (1). From the direct stiffness method in finite element analysis, the dynamic equilibrium of the system may be written in the following sub-matrix form:

$$\begin{bmatrix} [M_{ss}] & [0] & [0] \\ [0] & [M_{cc}] & [0] \\ [0] & [0] & [M_{mm}] \end{bmatrix} \begin{Bmatrix} \ddot{\vec{a}}_s \\ \ddot{\vec{a}}_c \\ \ddot{\vec{a}}_m \end{Bmatrix} + \begin{bmatrix} [C_{ss}] & [C_{sc}] & [0] \\ [C_{cs}] & [C_{cc}] & [C_{cm}] \\ [0] & [C_{mc}] & [C_{mm}] \end{bmatrix} \begin{Bmatrix} \dot{\vec{a}}_s \\ \dot{\vec{a}}_c \\ \dot{\vec{a}}_m \end{Bmatrix} + \begin{bmatrix} [K_{ss}] & [K_{sc}] & [0] \\ [K_{cs}] & [K_{cc}] & [K_{cm}] \\ [0] & [K_{mc}] & [K_{mm}] \end{bmatrix} \begin{Bmatrix} \vec{a}_s \\ \vec{a}_c \\ \vec{a}_m \end{Bmatrix} = \begin{Bmatrix} \vec{F}_s \\ \vec{F}_c \\ \vec{F}_m \end{Bmatrix} \tag{7}$$

where the characteristic matrices at the contact nodes are the sum of contribution from the structure (*s*) and the soil medium (*m*)

$$\begin{aligned} [M_{cc}] &= [M_{cc}^{(s)}] + [M_{cc}^{(m)}] \\ [C_{cc}] &= [C_{cc}^{(s)}] + [C_{cc}^{(m)}] \\ [K_{cc}] &= [K_{cc}^{(s)}] + [K_{cc}^{(m)}] \end{aligned} \tag{8}$$

Also in Eq. (7), $\vec{a}$ indicates the vector of absolute displacements of the structure. If both earthquake excitation and externally applied transient loading are considered, the right hand side of Eq. (7) can be expressed by corresponding nonzero terms. This force vector is included for completeness but is not completely considered in the numerical examples presented later in this paper. In this study, two different load conditions are taken into account: soil medium subjected to seismic waves only, consequently the external forces on the structure are set equal to zero in Eq. (7); and structures subjected to external loading only to investigate the effects of wave propagation in an elastic half-space.

3. Illustrative Numerical Analyses

The aforementioned methodology has been implemented in a two-dimensional time-domain *SE/FE* code in which, a library of spectral quadrilateral elements with various orders is coupled with frame (or, beam-column) finite elements. In order to validate the nature and general behavior of the method, some numerical examples have been considered. A plane strain condition of soil domain is assumed for all examples. No physical damping (i.e., pure elastic material behavior) is considered in all hybrid

analyses. Since a finite size of soil domain is regarded in the application of a domain type method such as *SEM*, a customary approach for dealing with infinite media consists of introducing truncated boundaries and setting fictitious absorbing conditions on them. To ensure that all energy arriving at the domain boundaries is absorbed, a special frequency independent non-reflecting viscous boundary condition has been widely used for various elastodynamic and soil-structure interaction problems [32-33]. To implement this boundary condition, two normal and tangential dashpots are defined at each node along the lateral and base boundaries of the soil domain. The normal dashpots are assigned to absorb the reflected compressive waves while the tangential ones are set to absorb the reflected shear waves. These dashpots must be placed far away from the initially disturbed region, as they are usually competent to transmit plane or cylindrical waves. Consequently, a large-scale domain should be discretized by *SEM*. Nevertheless, as shown in the following examples, *SEM* is capable to model a large-scale domain with considerably few degrees of freedom compared to other numerical methods. This feature of *SEM* compensates the necessity of modeling a large-scale domain, and let the approach to be still efficient.

3.1. Analysis of Elastic Half-Plane

As the first example, a linear elastic half-plane is examined to explain the applicability and accuracy of the present *SE* method, in calculating the free-field motion caused by vertical propagating incident *SV* wave of the Ricker type:

$$f(t) = f_{max}(1-2\tau^2)\,exp(-\tau^2)$$
$$\tau = 3\pi(t-0.5) \qquad (9)$$

where f_{max} is the maximum amplitude of the time history, which is selected as $0.0005m$ in this example, see Figure (2). Figure (3) represents the geometry used for this problem in which 25 spectral elements are considered. The material properties of the medium are: the shear wave velocity of the medium is $267m/s$, the mass density is $2.22t/m^3$, and the Poisson's ratio is 0.33.

To examine the convergence of *SE* modeling, three different discretized meshes are chosen. Each mesh consists of square spectral elements, see Figure (3), with a specific degree of Lagrange polynomials, n_ℓ. The time histories of horizontal displacement at the ground surface are investigated. The numerical results by *SEM* are compared with that of analytical solution, in the case of an incident *SV* wave. Figure (4) presents the results for three types of spectral elements inspected in this example.

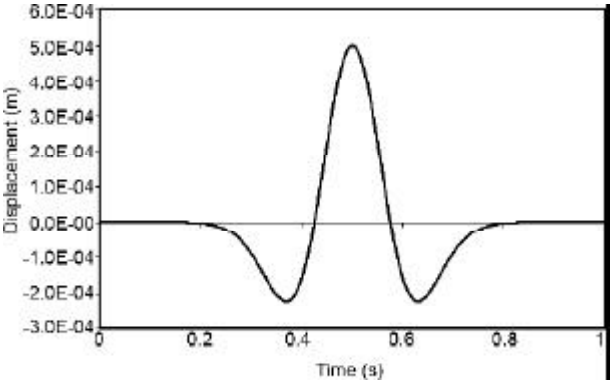

Figure 2. Load function time history of the incident wave (Ricker wavelet).

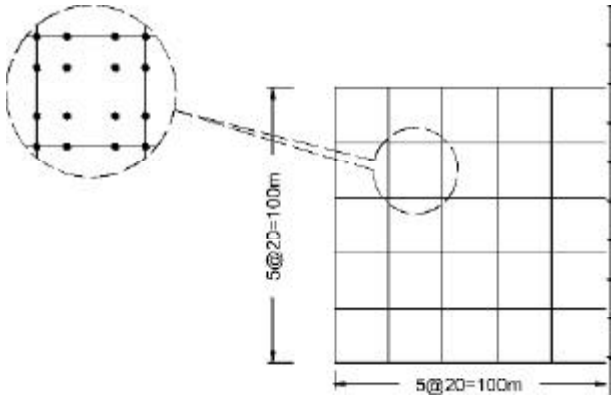

Figure 3. Geometry and discretization of the half-plane problem for which a typical third order (n_ℓ =3) spectral element is shown in more detail.

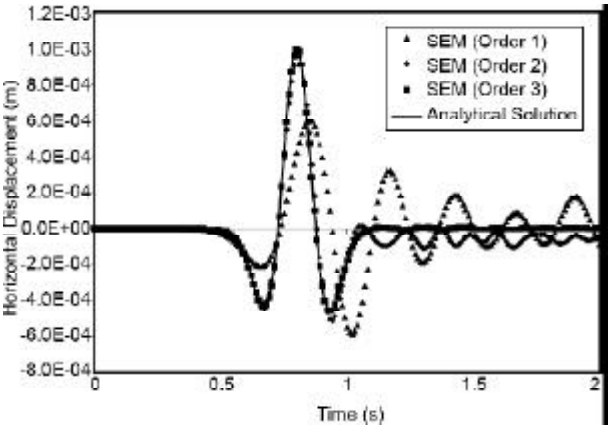

Figure 4. The SEM results of horizontal displacement time histories of the half-plane in the case of an incident SV wave for three types of spectral elements with specified order of Lagrange polynomials.

From Figure (4), one may easily observe that the higher-order elements give better results so that the results from the third order spectral elements and analytical approach are almost identical. As expected in the case of vertically propagating shear waves in an elastic half-plane, the total horizontal displacement of the free surface is twice the incident wave amplitude.

3.2. Analysis of Two-Layered Elastic Half-Plane

In this example, the application of the presented *SE* method in performing site response analysis of a two-layered half-plane is illustrated. In Figure (5), a soft layer with a height of $10m$ rests on a stiffer half-plane whose $50m$ in depth direction is modeled in this example. For this problem, the comparison of the results is made with the results based upon a hybrid *BE/FE* method [23]. Therefore, we selected the same geometry, see Figure (5), with the same shear wave velocities of $70.5m/s$ and $141m/s$ for the upper soft layer and the half-plane medium, respectively. Furthermore, the material properties of both layers are as follows: the Poisson's ratio is 0.33, and the mass density is $2.0ton/m^3$. The half-plane is excited by the same vertically incident *SV* wave as Figure (2). Similar to the first example, various meshes were inspected among which, the results corresponding to the converged mesh are presented here. These converged meshes are those of the minimum order that present the most accuracy in comparison with the hybrid *BE/FE* method [23]. The mesh includes 36 square spectral elements whose sides are shown in Figure (5).

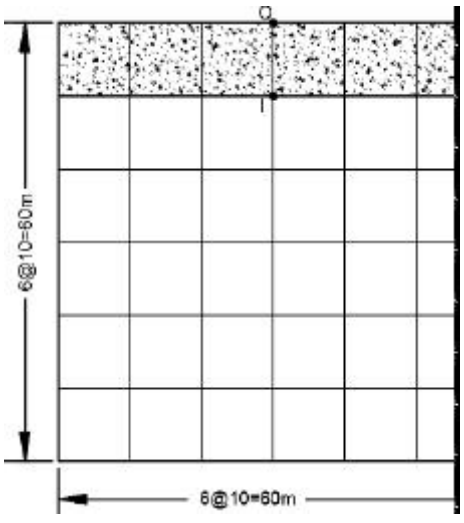

Figure 5. Geometry and discretization of the two-layered half-plane problem.

The time variation of horizontal displacement at points *O* and *I* are shown in Figures (6) and (7), respectively. Figures (8) and (9) present the horizontal acceleration time histories at the same points of Figures (6) and (7), respectively. As it is obvious

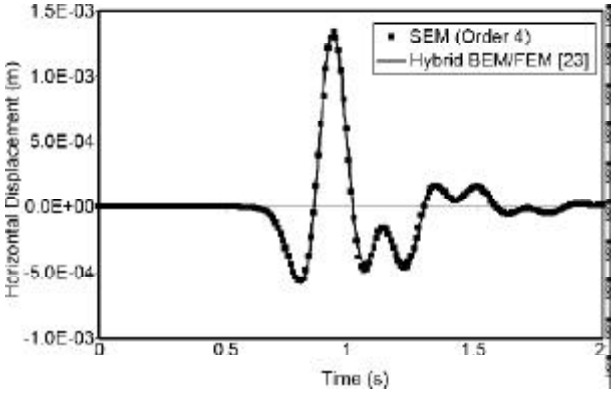

Figure 6. The SEM results of horizontal displacement time history at point O of the upper layer for the spectral elements of order 4.

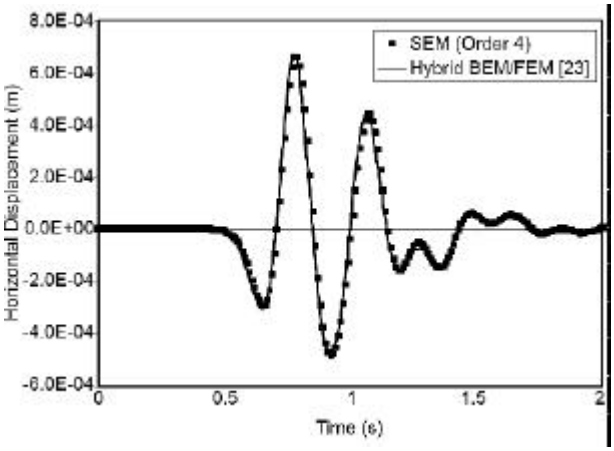

Figure 7. The SEM results of horizontal displacement time history at point I of the upper layer for the spectral elements of order 4.

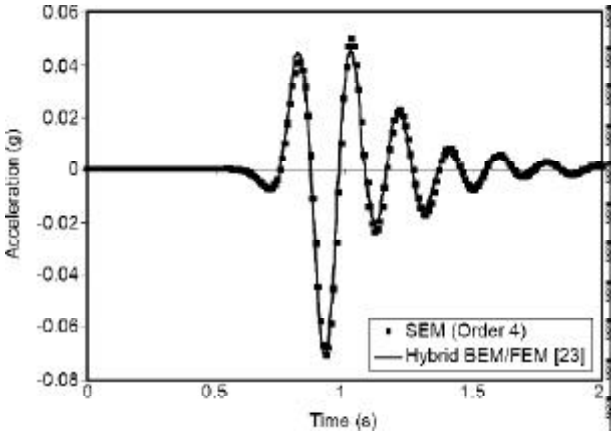

Figure 8. The SEM results of horizontal acceleration time history at point O of the upper layer for the spectral elements of order 4.

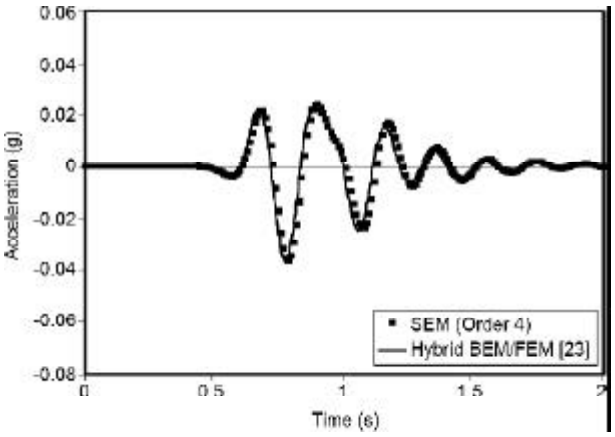

Figure 9. The SEM results of horizontal acceleration time history at point I of the upper layer for the spectral elements of order 4.

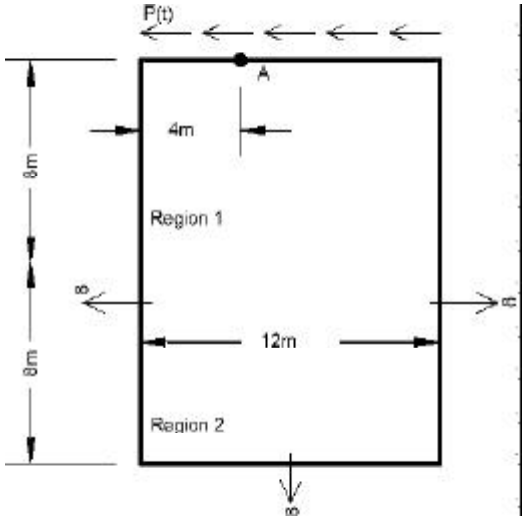

Figure 10. The considered geometry of a half-plane domain subjected to surface traction.

from these figures, excellent agreement can be observed between the results of the present work and the hybrid *BE/FE* method [23]. It is worthwhile remarking that the results shown in these figures are pertaining to very coarse meshes in which few degrees of freedom are involved.

3.3. Half-Plane Domain Subjected to Surface Traction

The response of a half-plane domain excited by a surface traction is examined in this example. Solutions based upon a *BE/FE* approach [34] are available for comparison. Figure (10) depicts the modeled elastic region, which is loaded by a uniformly-distributed ramp function, $\overline{P}(t)$, as:

$$\overline{P}(t)=\begin{cases} 0 & ; \quad t \le 0 \\ (\overline{P}_0 / Dt)t & ; \ 0 \le t \le Dt \\ \overline{P}_0 & ; \quad t \ge Dt \end{cases} \qquad (10)$$

in which, $\overline{P}_0$ is 1000*N/m*, and Δt is 0.0045 second. The material constants are as follows: the Young's modulus $E = 2.66\text{x}10^5 kN/m^2$, Poisson's ratio is 0.33, and the mass density is $2.0 ton/m^3$. In Ref. [34], the considered domain of Figure (10) was discretized into a *FE* subdomain (Region 1) and a *BE* subdomain (Region 2). In the present work, using a mesh consisting of 12 square spectral elements, *SEM* approach yields results, see Figure (11) which are almost identical to the results obtained by the *BE/FE* approach. It is worthwhile remarking that the results of *SEM* approach are pertaining to a simpler formulation in comparison with the formulation of the *BE/FE* approach.

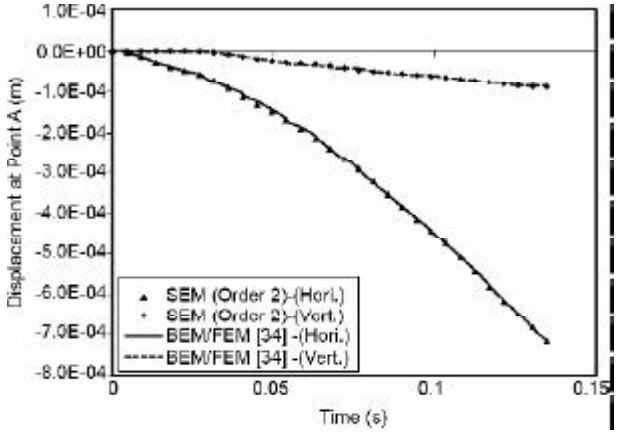

Figure 11. Horizontal and vertical components of displacement at observation point A due to a surface traction.

3.4. Single Degree of Freedom (DOF) Structure

The application of the present approach to the interaction between a flexible structure and its supporting elastic half-plane soil is examined in this example. The result of the present approach is compared with the lumped parameter approach [35] in which the supporting half-plane is replaced by equivalent dashpots and springs. Furthermore, the comparison of the results is made with the results based upon a hybrid *BE/FE* method [21]. Figure (12) represents the single degree of freedom stick model of the structure and its supporting half-plane. The same material properties of Ref. [21] are selected as follows: the Lame' constants $\lambda = 24081$ and $\mu = 16054$, and the mass density of the elastic half-plane is 0.002006. Furthermore, the lumped mass is equal to 10 and is located at the story level with the height of $L = 3$. The lateral

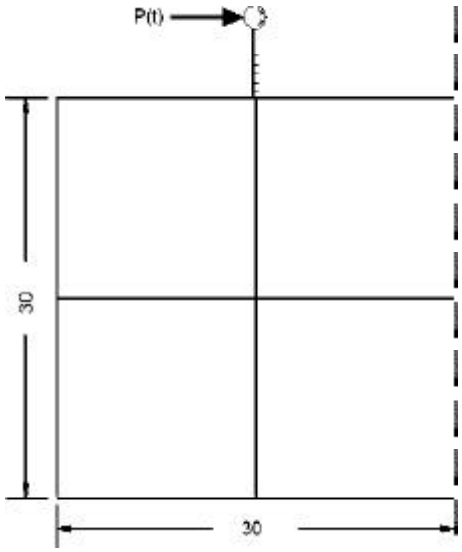

Figure 12. Geometry and discretization of the 1DOF lumped mass structure resting on an elastic half-plane.

rigidity of the structure is $EI = 1.8\text{x}10^6$; all quantities in consistent units. The right hand side of Eq. (7) is modified as the following form to represent the applied harmonic horizontal excitation at the mass level

$$\begin{Bmatrix} \vec{F}_s \\ \vec{F}_c \\ \vec{F}_m \end{Bmatrix} = \begin{Bmatrix} P(t) \\ \vec{0} \\ \vec{0} \end{Bmatrix}; \quad P(t) = sin(14.14t) \tag{11}$$

The response of the structure is obtained using a mesh including four square spectral elements to model the elastic half-plane, and one frame finite element for the single *DOF* structure. The results corresponding to fourth and fifth degree of Lagrange polynomials ($n_\ell = 4$ and 5) are represented in Figure (13). As may be observed from these figures, good agreement between the results of the proposed *SE/FE* approach and the results obtained by the *BE/FE* [21] and simplified [35] approaches indicates the validity of the present algorithm.

3.5. Two Degrees of Freedom Structure

In this example, the application of the hybrid *SE/FE* approach to the interaction between a flexible two degrees of freedom structure and its supporting half-plane medium is investigated. The result of the present approach is compared with the results of a hybrid *BE/FE* method [21].

Figure (14) represents the two *DOF* stick model of the structure and its supporting half-plane. The

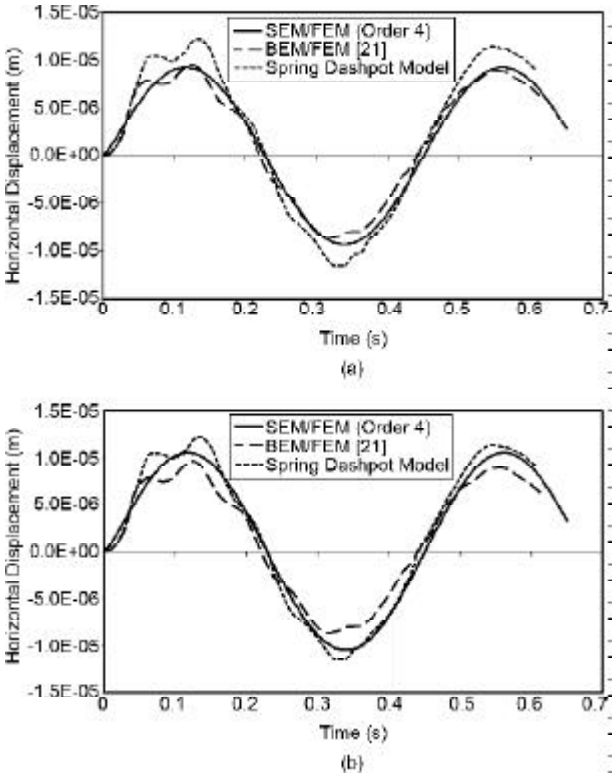

Figure 13. Time variations of horizontal displacement at the level of lumped mass: (a) fourth order and (b) fifth order spectral elements are used for comparison of three methods.

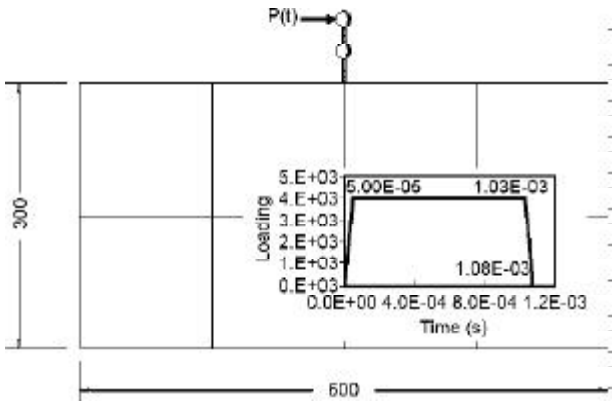

Figure 14. Geometry, discretization, and applied loading of the 2DOF lumped mass structure resting on an elastic half-plane.

same material properties of Ref. [21] are chosen as follows: the Lame constants λ = 6629990 and μ = 3315000, and the mass density of the elastic half-plane is 0.000282. Moreover, the lumped masses of each degree of freedom are equal to 10 and are located at the story levels with the height of $L = 12$. The lateral rigidity of the structure is $EI = 1.55\text{x}10^{12}$; all quantities in consistent units. No structural damping is considered in this example. For this example, the right hand side of Eq. (7) is modified

as the following form to represent the trapezoidal excitation, see the inset of Figure (14), applied at the top mass level

$$\begin{Bmatrix} \vec{F}_s \\ \vec{F}_c \\ \vec{F}_m \end{Bmatrix} = \begin{Bmatrix} \vec{F}_s(t) \\ \vec{0} \\ \vec{0} \end{Bmatrix}; \qquad \vec{F}_s(t) = \begin{Bmatrix} P(t) \\ 0 \end{Bmatrix} \tag{12}$$

The response of this structure is computed using a mesh of eight square spectral elements to model the elastic half-plane, and two frame finite elements for the 2*DOF* structure. The response of the soil-structure system is firstly obtained using a fixed base analysis to validate the *FEM* formulation of the present approach, see Figure (15). As expected, this analysis represents the condition in which the structure experiences undamped oscillations in the initial period of 1.08*ms* (forced vibration) followed by the rest period (free vibration) of the response. For the whole soil-structure system, the horizontal displacements of the first and second lumped masses corresponding to $n_\ell = 2$ are represented in Figure (16). As can be seen from this figure, the general trend of two approaches presents a reasonable agreement from engineering point of view. The discrepancy between two approaches may be attributed to the following features:

a) The proposed *SE/FE* approach is two-dimensional, whereas the *BE/FE* approach [21] is three-dimensional, and
b) The principle difference between the *SE* and *BE* formulation of the present approach and the *BE/FE* one, respectively.

3.6. Five Story Frame Structure

In the last example, the application of the proposed approach to a more practical problem of interaction between a typical two-span five-story frame consisting of twenty-five frame finite elements and its supporting half-plane soil is studied, see Figure (17). The following properties are selected for all structural elements: lateral rigidity $EI = 2.52 \times 10^{10}$, mass density $\rho = 6000$, and cross-section area

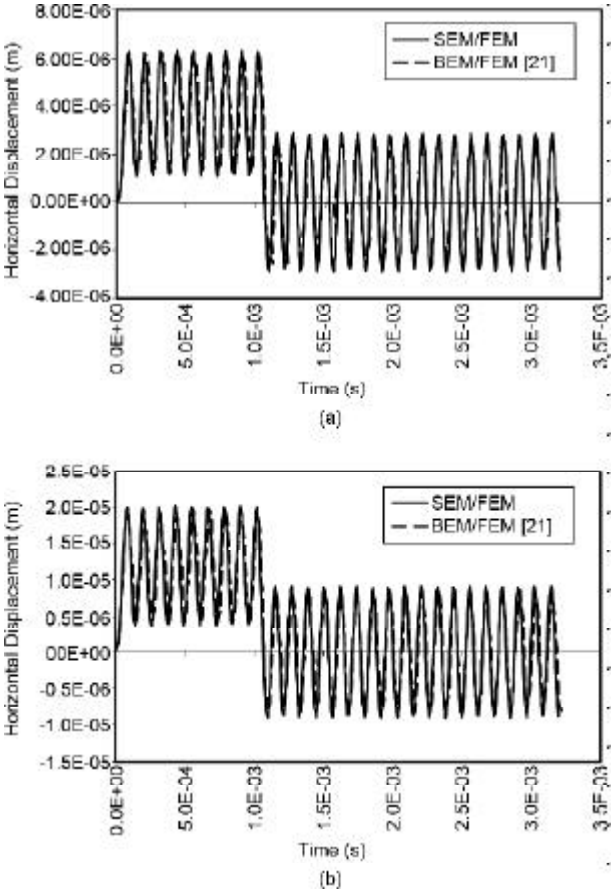

Figure 15. Horizontal displacement time histories of the fixed base 2DOF structure at (a) the first and (b) the second lumped mass levels.

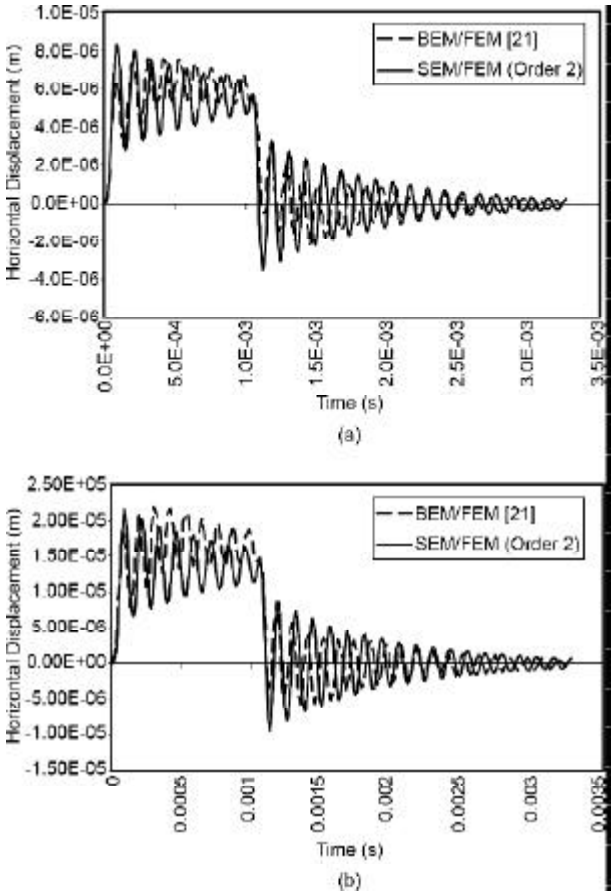

Figure 16. The coupled SEM/FEM results of horizontal displacement time histories at (a) the first and (b) the second lumped mass levels.

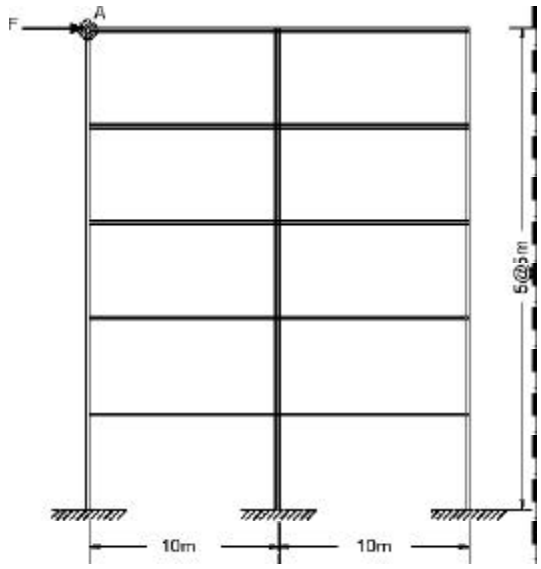

Figure 17. Geometry and applied loading (at point A) of the two-span five-story frame structure.

$A = 1.00$, all quantities in consistent units. No structural damping is considered in this example. In addition, the following parameters are used for half-plane medium: $EI = 2.6 \times 10^9$, $\rho = 2000$, and $v = 0.33$. Figure (18) depicts the structural system, excited by a concentrated horizontal loading, see the inset of Figure (18), resting on a half-plane which consists of fourteen spectral elements $(20 \times 70 m^2)$ with a certain degree of Lagrange.

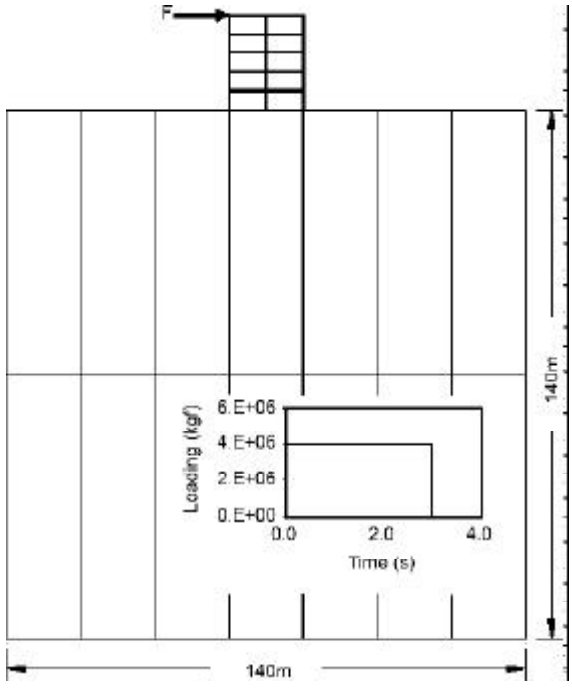

Figure 18. Geometry, discretization, and applied loading of the two-span five-story frame structure and its beneath elastic half-plane.

In order to show the convergence of results towards an exact solution, various meshes associated to n_ℓ = 4, 6 and 8 are inspected whose results are presented in Figure (19). This figure indicates that the result corresponding to $n_\ell = 8$ represents the converged values of horizontal displacement. Furthermore, as this method considers soil-structure interaction effects, damped motion of the structure response due to the radiation damping in the half-plane is clearly observed. In addition, the efficiency of the viscous boundary condition employed in the present research is examined in Figure (20). Obviously, the results of fixed (or, without viscous dampers) boundary conditions show significant errors due to the problem of wave reflection on the far-field boundaries of the half-plane domain.

To compare the responses of the soil-structure system according to variations in the stiffness of half-plane domain, a time history analysis for different Young's modulus is carried out using the proposed hybrid approach.

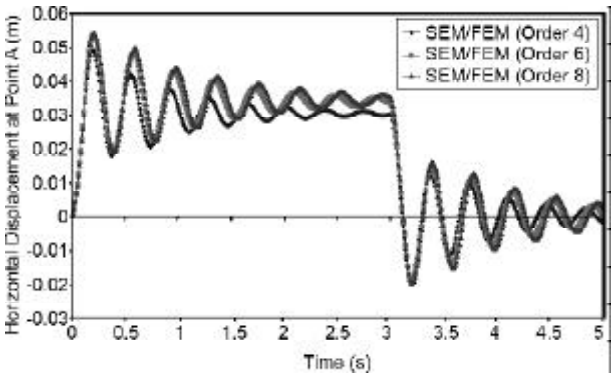

Figure 19. The horizontal displacement time histories at the fifth story level (point A) for three types of spectral elements with specified order of Lagrange polynomials.

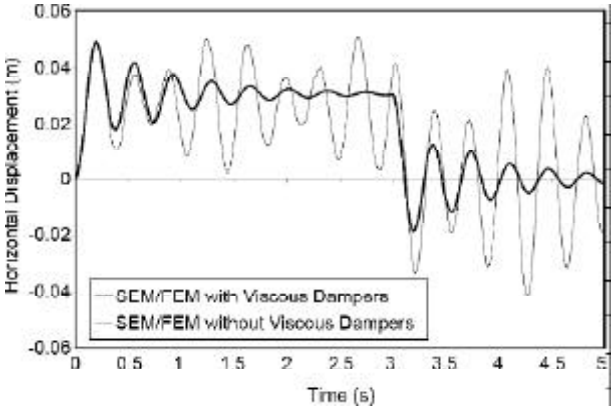

Figure 20. The horizontal displacement time histories of point A for two cases of far-field boundary conditions.

Figure (21) shows the plots of time histories of horizontal displacement at the fifth story level for various Young's modulus of soil medium. It is observed that, as the Young's modulus of half-plane decreases, the effect of soil-structure interaction on the response of whole system is more considerable. Moreover, this effect considerably increases the natural frequency of whole system, as expected.

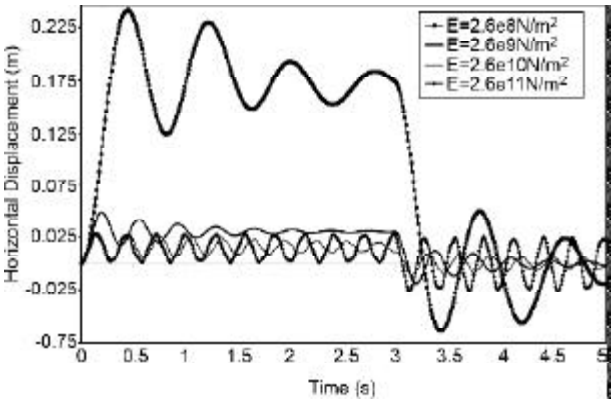

Figure 21. The horizontal displacement time histories at the fifth story level (point A) for various Young's modulus of half-plane medium.

4. Conclusions

The present research proposes a hybrid high-order (*SEM*)-low-order (*FEM*) formulation for the transient analysis of interaction of soil-structure coupled media. As realized from the detailed *SEM* formulation, the only discrepancies between *SEM* and classical *FEM* could be summarized in three features: adoption of specific high-order shape functions, specific integration rule, and the nature of the time-marching scheme. These special features enable *SEM* to overcome some inherent difficulties of other numerical methods (e.g., *FEM* and *BEM*) for which, illustrative discussions have been provided in this paper. In the proposed approach, the finite domain, which would be considered as the structure, is represented by *FEM* and the half space medium of soil is modeled by *SEM*. Dynamic mass, damping, and stiffness matrices corresponding to related domains of the *SSI* system are derived and combined by using direct method. Several numerical studies are performed to verify and examine the applicability of the hybrid model and the developed computer program. Comparison is made among different analytical and numerical (e.g., *FEM* and *BEM*) approaches to show that the selected problems may be successfully modeled with few number of *DOFs*, preserving high accuracy and efficiency.

Further development of the proposed method is necessary, as this method will be much more efficient for the analysis of large three-dimensional domains. Moreover, this method has the advantage over other numerical methods in that it provides a direct time domain approach of obtaining the time history of the response. Using this advantage, the new *SE/FE* method is appropriate to handle non-linearities and inhomogeneities of soil domain. The aforementioned extensions of the present method are under investigation whose results will be offered in a future publication.

References

1. Wolf, J.P. (1995). "Dynamic Soil-Structure Interaction", Prentice-Hall, NJ.

2. Wolf, J.P. and Song, C. (2002). "Some Cornerstones of Dynamic Soil-Structure Interaction", *Engineering Structures*, **24**, 13-28.

3. Chopra, A.K. and Chakrabarti, P. (1981). "Earthquake Analysis of Concrete Gravity Dams Including Dam-Water-Foundation Rock Interaction", *Earthquake Engineering and Structural Dynamics*, **9**(4), 363-383.

4. Mroueh, H. and Shahrour, I. (2003). "A Full 3-D Finite Element Analysis of Tunneling-Adjacent Structures Interaction", *Computers and Geotechnics*, **30**, 245-253.

5. Ju, S.H. (2003). "Evaluating Foundation Mass, Damping and Stiffness by the Least-Squares Method", *Earthquake Engineering and Structural Dynamics*, **32**(9), 1431-1442.

6. Maki, T., Maekawa, K., and Mutsuyoshi, H. (2006). "RC Pile-Soil Interaction Analysis Using a 3D-Finite Element Method with Fibre Theory-Based Beam Elements", *Earthquake Engineering and Structural Dynamics*, **35**(13), 1587-1607.

7. Guddati, M.N. and Tassoulas, J.L. (1999). "Space-Time Finite Elements for the Analysis of Transient Wave Propagation in Unbounded Layered Media", *International Journal of Solids and Structures*, **36**, 4699-4723.

8. Basu, U. and Chopra, A.K. (2002). "Numerical Evaluation of the Damping-Solvent Extraction Method in the Frequency Domain", *Earthquake Engineering and Structural Dynamics*, **31**(6), 1231-1250.

9. Kim, D.K. and Yun, C. (2003). "Earthquake Response Analysis in the Time Domain for 2D Soil-Structure Systems Using Analytical Frequency-Dependent Infinite Elements", *International Journal for Numerical Methods in Engineering*, **58**(12), 1837-1855.

10. Zerfa, Z. and Loret, B. (2003). "A Viscous Boundary for Transient Analyses of Saturated Porous Media", *Earthquake Engineering and Structural Dynamics*, **33**(1), 89-110.

11. Lysmer, J. and Drake, L.A. (1972). "A Finite Element Method for Seismology", In: Bolt, B.A., Editor, Methods in Computational Physics, Academic Press Inc.

12. Toshinawa, T. and Ohmachi, T. (1992). "Love Wave Propagation in Three-Dimensional Sedimentary Basin", Bulletin of Seismological Society of America, **82**, 1661-1667.

13. Shakib, H. and Fuladgar, A. (2004). "Dynamic Soil-Structure Interaction Effects on the Seismic Response of Asymmetric Buildings", *Soil Dynamics and Earthquake Engineering*, **24**, 379-388.

14. Marfurt, K.J. (1984). "Accuracy of Finite-Difference and Finite-Element Modeling of the Scalar Wave Equations", *Geophysics*, **49**, 533-549.

15. Karabalis, D.L. and Mohammadi, M. (1998). "3-D Dynamic Foundation-Soil-Foundation Interaction on Layered Soil", *Soil Dynamics and Earthquake Engineering*, **17**, 139-152.

16. Pak, R.Y.S. and Guzina, B.B. (1999). "Seismic Soil-Structure Interaction Analysis by Direct Boundary Element Methods", *International J. of Solids and Structures*, **36**, 4743-4766.

17. Karabalis, D.L. (2004). "Non-Singular Time Domain BEM with Applications to 3D Inertial Soil-Structure Interaction", *Soil Dynamics and Earthquake Engineering*, **24**, 281-293.

18. Chuhan, Z., Feng, J., and Pekau, O.A. (1995). "Time Domain Procedure of FE-BE-IBE Coupling for Seismic Interaction of Arch Dams and Canyons", *Earthquake Engineering and Structural Dynamics*, **24**, 1651-1666.

19. Yazdchi, M., Khalili, N., and Valliappan, S. (1999). "Dynamic Soil-Structure Interaction Analysis Via Coupled Finite-Element-Boundary-Element Method", *Soil Dynamics and Earthquake Engineering*, **18**(7), 499-517.

20. Von Estorff, O. and Firuziaan, M. (2000). "Coupled BEM/FEM Approach for Nonlinear Soil-Structure Interaction", *Engineering Analysis with Boundary Elements*, **24**, 715-725.

21. Rizos, D.C. and Wang, Z. (2002). "Coupled BEM-FEM Solutions for Direct Time Domain Soil-Structure Interaction Analysis", *Engineering Analysis with Boundary Elements*, **26**, 877-888.

22. Almeida, V.S. and De Paiva, J.B. (2004). "A Mixed BEM-FEM Formulation for Layered Soil-Superstructure Interaction", *Engineering Analysis with Boundary Elements*, **28**, 1111-1121.

23. Kamalian, M., Jafari, M.K., Sohrabi-Bidar, A., Razmkhah, A., and Gatmiri, B. (2006). "Time-Domain Two-Dimensional Site Response Analysis of Non-Homogeneous Topographic Structures by a Hybrid BE/FE Method", *Soil Dynamics and Earthquake Engineering*, **26**, 753-765.

24. Liingaard, M., Andersen, L., and Ibsen, L.B. (2007). "Impedance of Flexible Suction Caissons", *Earthquake Engineering and Structural Dynamics*, **36**, 2249-2271.

25. Fischer, P.F. and Ronquist, E.M. (1994). "Spectral-Element Methods for Large Scale Parallel Navier-Stokes Calculations", *Computer Methods in Applied Mechanics and Engineering*, **116**, 69-76.

26. Faccioli, E., Maggio, F., Quarteroni, A., and Tagliani, A. (1996). "Spectral-Domain Decom-

position Methods for the Solution of Acoustic and Elastic Wave Equations", *Geophysics*, **61**(4), 1160-1174.

27. Komatitsch, D., Vilotte, J.-P., Vai, R., Castillo-Covarrubias, J.M., and Sanchez-Sesma, F.J. (1999). "The Spectral Element Method for Elastic Wave Equations - Application to 2-D and 3-D Seismic Problems", *International Journal for Numerical Methods in Engineering*, **45**, 1139-1164.

28. Casadei, F., Gabellini, E., Fotia, G., Maggio, F., and Quarteroni, A. (2002). "A Mortar Spectral/ Finite Element Method for Complex 2D and 3D Elastodynamic Problems", *Computer Methods in Applied Mechanics and Engineering*, **191**, 5119-5148.

29. Chiaruttini, C., Grimaz, S., and Priolo, E. (1996). "Modelling of Ground Motion in the Vicinity of Massive Structures", *Soil Dynamics and Earthquake Engineering*, **15**, 75-82.

30. Patera, A.T. (1984). "A Spectral Element Method for Fluid Dynamics: Laminar Flow in a Channel Expansion", *J. of Computational Physics*, **54**, 468-488.

31. Zienkiewicz, O.C. and Taylor, R.L. (2000). "The Finite Element Method", Butterworth and Heinmann, Oxford.

32. Lysmer, J. and Kuhlemeyer, R.L. (1969). "Finite Dynamic Model for Infinite Media", *ASCE Journal of Engineering Mechanics*, **95**, 859-877.

33. White, W., Valliappan, S., and Lee, I.K. (1977). "Unified Boundary for Finite Dynamic Models", *ASCE Journal of Engineering Mechanics*, **103**(5), 949-964.

34. Von Estorff, O. and Prabucki, M.J. (1990). "Dynamic Response in the Time Domain by Coupled Boundary and Finite Elements", *Computational Mechanics*, **6**, 35-46.

35. Wolf, J.P. (1994). "Foundation Vibration Analysis Using Simple Physical Models", Prentice-Hall, Englewood Cliffs, NJ.